Evaluation of an Enhanced Graded Precision Localization Algorithm for Wireless Sensor Networks

BAMULI SWAPNA[1], T.RAJINIKANTH[2]
[1,2] *Assistant Professor, Vaagdevi Degree& Pg College, Hanamkonda, Telangana-506001*

ABSTRACT: **This paper introduces an enhanced version of the graded precision localization algorithm, GRADELOC, named IGRADELOC. The performance of GRADELOC is influenced by the regions created through the overlapping radio ranges of nodes within the underlying sensor network. Variations in these regional patterns can significantly impact the accuracy and nature of localization. IGRADELOC proposes two key improvements to address these limitations. First, adjustments to the radio range of fixed-grid nodes are introduced, considering the actual radio range of commonly available nodes. These adjustments facilitate routing through these nodes, a critical aspect overlooked by GRADELOC but essential for deploying any ad hoc network, particularly sensor networks. A theoretical model is presented, linking the radio range to the grid infrastructure's cell dimensions, enabling deployment plans that achieve the desired precision for coarse-grained localization. Second, it is noted that fine-grained localization in GRADELOC does not yield substantial performance gains compared to coarse-grained localization. To address this, IGRADELOC introduces a tunable parameter designed to enhance the precision of fine-grained localization, ensuring improved overall performance.**

KEYWORDS: ***Wireless Sensor Networks, Positioning, Centroid Method, Time Difference of Arrival (TDOA), Fixed-Grid Approach***

1. INTRODUCTION

The GRADELOC algorithm, introduced in utilizes three key localization techniques: (a) centroid-based computation for coarse-grained localization, (b) time difference of arrival (TDOA) for fine-grained localization, and (c) last-mile localization supported by a mobility module. The mobility module incorporates (i) an accelerometer to calculate displacement using steps and stride lengths, and (ii) a gyroscope and magnetic compass combination for determining motion direction. Nodes requiring localization, termed NTLs, are categorized into three types: coarse-grained NTLs (CG-NTLs), fine-grained NTLs (FG-NTLs), and extra-fine-grained NTLs (EFG-NTLs). CG-NTLs rely solely on (a), FG-NTLs use (a) and (b), while EFG-NTLs employ all three techniques (a, b, and c), thereby achieving graded precision localization with the same GRADELOC algorithm.

GRADELOC's effectiveness is governed by two factors: the precision requirements of the NTL and the transmission range of grid nodes that form the sensor network infrastructure. Each grid intersection hosts an energy-unconstrained reference node set (REFN) consisting of two nodes: REFN0, for periodic beaconing, and REFN1, for TDOA-based fine-grained localization. REFN0 nodes periodically broadcast location beacons to assist localization, while REFN1 nodes respond to explicit fine-grained localization requests, operating on principles outlined.The transmission range of REFN0 nodes segments the grid into regions, with each covered by a distinct set of REFN0 nodes. As the NTL moves, it collects REFN0 beacons and, at regular intervals (centroid computation intervals), calculates its location by computing the centroid of locations associated with beacons exceeding a predefined threshold. This centroid serves as the advertised location for CG-NTLs. For FG-NTLs, if the new centroid differs from the previous one, fine-grained localization is triggered using REFN1 nodes. EFG-NTLs enhance this process by continuously estimating their location through the mobility module between fine-grained localization operations.

However, in GRADELOC, the transmission range of REFN0 nodes, illustrated in Fig. 3, does not overlap with neighboring REFN0 nodes, preventing communication of estimated locations to a central gateway. Additionally, the frequent change in the candidate REFN0 set (nodes meeting the beacon threshold) limits the cost-performance trade-off, as the communication overhead of fine-grained localization often outweighs the gains in precision. To address these issues, IGRADELOC introduces improvements to enhance localization efficiency and precision, providing a refined solution to the limitations observed in GRADELOC.

2. THE IGRADELOC ALGORITHM

The flow diagram of IGRADELOC, shown in Fig. 2, maintains the three NTL variants: CG-NTL, FG-NTL, and EFG-NTL. Their corresponding parameter sets (coarseGrained, fineGrained, selfLocalize) are initialized according to the configuration outlined in Table 1.

3. TOPOLOGY

The topology employed by IGRADELOC, identical to that of GRADELOC, consists of a 5x5 grid of fixed nodes, where each node is a set comprising REFN0 and REFN1, as illustrated in Fig. 1. However, IGRADELOC enhances the transmission range of REFN0 nodes, as depicted in Fig. 4. Unlike the range in Fig. 3 of GRADELOC, this extended range ensures neighboring nodes remain within each other's coverage, enabling routing through the grid nodes. The transmission range of a REFN0 node is represented by RR, while the side length of a square grid cell is denoted as LL. Although R≥LR \geq L is a necessary condition for routing, Section 4 explains why this alone may not guarantee the successful operation of IGRADELOC.

Table1: Node Classification

NTL	Coarse Grained	Fine Grained	Self Localize
None	False	False	False
CG-NTL	True	False	False
FG-NTL	True/False	True	False
EFG-NTL	True/False	True	True

4. THEORETICAL FOUNDATIONS

In this section, we establish the criteria for selecting the optimal parameter values for IGRADELOC's operation. The subsequent sections address challenges related to creating a deployment scenario for IGRADELOC. The following assumptions are made:

1. Fine-grained localization using TDOA performs effectively when the NTL moves at a low speed. Since this study compares various localization methods, the NTL is assumed to move at a constant low speed, as defined by the mobility model detailed in Section 8.3.
2. Both REFN0s and NTLs are implemented using the same sensor nodes. Therefore, all discussions concerning node characteristics, such as radio range, are applicable to both REFN0s and NTLs.

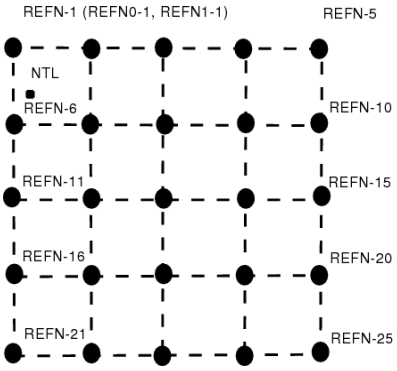

Figure1:5x5REFNsarrangedinagrid

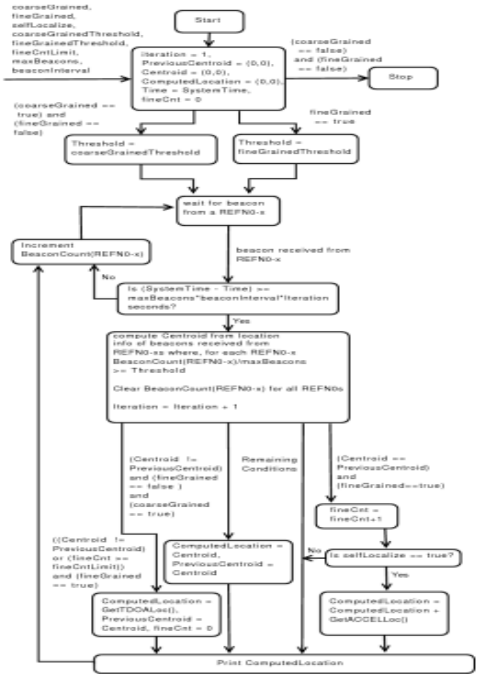

Figure 2: Flow diagram of IGRADELOC algorithm

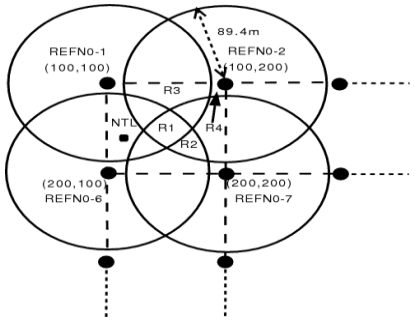

Figure3: GRADELOC Radio Range

5. RELATIONSHIP OF DISTANCE BETWEEN GRID NODES AND NODE RANGE

When an FG-NTL decides to perform fine-grained localization (FGL), it must reach at least three non-

collinear REFN1 nodes. We propose that for the NTL to access three non-collinear fixed nodes within one hop distance, its transmission range while moving within the fixed grid must be at least L5/2L\sqrt{5}/2.

Proof: Consider a grid cell ABCD (with a side length of LL) from the fixed grid, as shown in Fig. 5. The diagonals AC and BD, along with the perpendicular bisectors EG and FH of the opposite sides, divide the square into eight congruent triangles (P1,...,P8).

1. Let pip_i and pjp_j be two points within the square ABCD. The lines EG and FH are the perpendicular bisectors of the opposite sides, and II represents the center of the square.
2. Let SS be a set of points {p1,p2,...,pN}\{ p_1, p_2, ..., p_N \}, with pi,pj∈Sp_i, p_j \in S. D(pi,pj)D(p_i, p_j) is the distance between points pip_i and pjp_j, and M(pi,pj)=max⁡{D(pk,pj)}M(p_i, p_j) = \max \{ D(p_k, p_j) \} for all pk∈Sp_k \in S, where 1≤k≤N1 \leq k \leq N.
3. Let X={all points in ΔAIE}X = \{ \text{all points in } \Delta AIE \}.
4. For all pi∈Xp_i \in X, clearly, M(pi,pA)=D(pi,pA)M(p_i, p_A) = D(p_i, p_A) (hypotenuse), which equals L5/2L \sqrt{5} / 2, denoted as L1L_1.
5. Let Y1={all points in ΔBAE}Y_1 = \{ \text{all points in } \Delta BAE \}. For all pi∈Y1p_i \in Y_1, clearly, M(pi,pB)=D(pi,pB)M(p_i, p_B) = D(p_i, p_B) (hypotenuse), which also equals L5/2L \sqrt{5} / 2, denoted as L2L_2. Let Y2={all points in ΔBGE}Y_2 = \{ \text{all points in } \Delta BGE \}. For all pi∈Y2p_i \in Y_2, M(pi,pB)=D(pi,pB)M(p_i, p_B) = D(p_i, p_B) (hypotenuse), so X⊆Y1∪Y2X \subseteq Y_1 \cup Y_2. Therefore, for all pi∈X∪{pB}p_i \in X \cup \{ p_B \}, M(pi,pB)=D(pi,pB)M(p_i, p_B) = D(p_i, p_B), denoted by L2L_2.
6. Let Z={all points in ΔAID}Z = \{ \text{all points in } \Delta AID \}, and for all pi∈Zp_i \in Z, M(pi,pD)=D(pi,pD)M(p_i, p_D) = D(p_i, p_D) (hypotenuse). Since X⊆ZX \subseteq Z, for all pi∈X∪{pD}p_i \in X \cup \{ p_D \}, M(pi,pD)=D(pi,pD)M(p_i, p_D) = D(p_i, p_D), denoted by L3L_3.

From steps 4, 5, and 6, we conclude that the three fixed REFN0 nodes at A, B, and D are within one hop of an NTL at position pip_i, where pi∈Xp_i \in X, provided the NTL's range is at least max⁡(L1,L2,L3)=L2=L5/2\max(L_1, L_2, L_3) = L_2 = L \sqrt{5} / 2. By symmetry, this relation holds for each of the triangles P1,...,P8P_1, ..., P_8.

Therefore, there are at least three REFN0 nodes within one hop of an NTL moving within a grid cell, provided the NTL's range is ≥L5/2\geq L \sqrt{5} / 2.

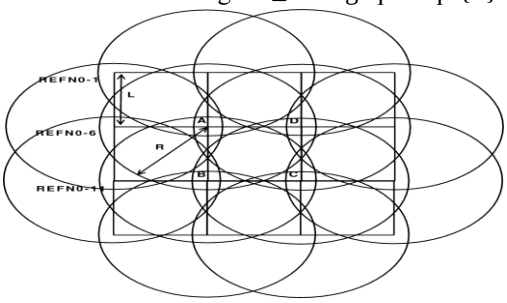

Figure4: IGRADELOC Radio Range

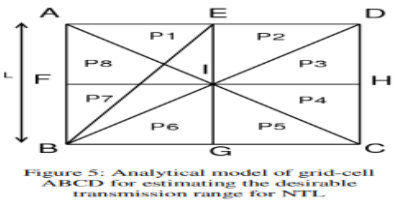

Figure 5: Analytical model of grid-cell ABCD for estimating the desirable transmission range for NTL

Figure5: Analyticalmodelofgrid-cell ABCD for estimating the desirable transmission range for NTL

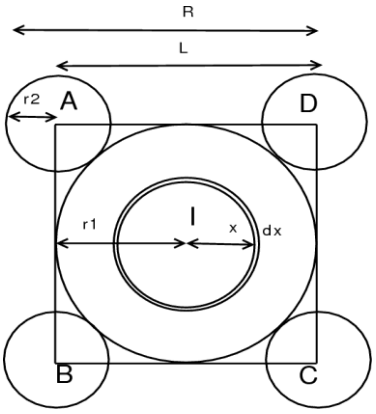

Figure6:Analytical model of grid-cell ABCD for estimating localization error

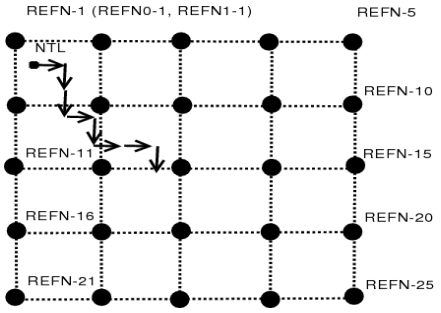

Figure7: NTL mobility model

6. ANALYTICAL ERROR ESTIMATION MODEL FOR COARSE-GRAINED LOCALIZATION

Fig. 4 illustrates a typical deployment scenario for IGRADELOC, where the range of each REFN0 and NTL is L5/2L \sqrt{5}/2, as explained in Section 5, and the side length of each square cell is LL. For analysis, we approximate the cell ABCD in Fig. 4 using the regions shown in Fig. 6. A circle centered at KK with a radius LL is denoted as CK,LC_{K,L}. In Fig. 6, the radius of CIC_I is r1=L/2r_1 = L/2, and the radius of CAC_A, CBC_B, CCC_C, and CDC_D is r2=R−Lr_2 = R - L. Let SESE represent the set of estimated locations {E1,E2,...,EN}\{ E_1, E_2, ..., E_N \} of an NTL (obtained by computing the centroid of received beacons in coarse-grained localization), and SA={A1,A2,...,AN}SA = \{ A_1, A_2, ..., A_N \} be the corresponding set of actual locations. The cumulative localization error (CLE) and the mean absolute error (MAE) of CLE are defined as follows:

$$CLE=\sum_{i=1}^{i=N} |E_i-A_i| \quad (1)$$

$$MAE(CLE)=CLE/N \quad (2)$$

Calculating the localization error for an NTL located anywhere within the four quarter circles at each corner inside the grid cell ABCD is equivalent to calculating it for one of the circles, such as CA,r2C_A, r_2. The areas of CI,r1C_I, r_1 and CA,r2C_A, r_2 together account for approximately 82% of the square's total area. Therefore, estimating the coarse-grained localization error within these regions can be used to roughly determine the overall coarse-grained localization error across the entire grid.

Region 1: The centroid of ABCD is II. The estimated location EiE_i (calculated by receiving beacons from grid nodes A, B, C, D) for an NTL at any point pi∈CI,r1p_i \in C_{I,r1} is II (the center). For an NTL located at a point pip_i on the circumference of circle CI,xC_{I,x}, the cumulative localization error (CLE) is given by CLE=(circumference of CI,x)×(radius of CI,x)=2πx ×x\text{CLE} = \text{(circumference of } C_{I,x}) \times \text{(radius of } C_{I,x}) = 2\pi x \times x. By integrating over CI,r1C_{I,r1}, the cumulative localization error for an NTL located anywhere inside CI,r1C_{I,r1}, denoted as CLE1, is given by:

$$CLE_1=\int_0^{r1} 2\pi x^2 dx=2\pi (r1)^3/3 \quad (3)$$

wherer1=L/2andnumberofpointsdenotedbyN_1isnothingbutthereaofC$_{I,r1}=\pi(r1)^2$

Region2: Similarly, the cumulative localization error for an NTL present anywhere in $C_{A,r2}$ denoted by CLE_2 is given by

$$CLE_2=\int_0^{r2} 2\pi x^2 dx=2\pi(r2)^3/3 \quad (4)$$

wherer2=(R−L)andcorrespondingnumberofpoints denotedN_2istheareaof$C_{A,r2}=\pi(r2)^2$. Putting the lower bound of the desirable range R = L√5/2 of an NTL, we get

$$MAE=(CLE_1+CLE_2)/(N_1+N_2)=0.32L(approx.) \quad (5)$$

7. SELECTING BEACONS AND CENTROID COMPUTATION INTERVALS

Let the centroid be computed every PP seconds, and the beacon interval be pp seconds. A granularity function G(p,P)=p/PG(p,P) = p/P is defined, with a threshold TT for an NTL to select a REFN0 as a candidate for centroid computation, given by T=G(p,P)·nT = G(p,P) \cdot n, where nn belongs to the set of positive integers such that 0<n·p/P≤10 < n \cdot p / P \leq 1. We use Fig. 6 to analyze the values of the various parameters, as they correspond to homogeneous (circular) spaces that form significant portions of the mobility area (Section 6), and the centroid computed by an NTL is simply the center of the respective circles. To ensure the centroid computation is invoked within these spaces, the centroid computation interval PP is taken as:

$$P=\min\{r1,r2\}/S=(\sqrt{5}/2-1)L/S \quad (6)$$

where S is the maximum speed of the NTL. Accordingly, p is chosen so that G(p,P) = 0.1 and that $1 \leq n \leq 10$. The parameter*maxBeacons* in Fig. 2 refers to maximum value that could be taken byn. So *maxBeacons* has avalueof 10. Parameter *beaconInterval*is nothingbut p.

1. Fine-grained localization with TDOA

An FG-NTL or EFG-NTL invokes the GetTDOALoc() function (see Fig. 2) for fine-grained localization. To initiate this process, the NTL broadcasts a beacon indicating its current location, alerting at least three REFN1 nodes (as explained in Section 5) that fine-grained localization (FGL) is requested. The results of TDOA-based localization, as discussed in [3], use Taylor series and Fang's

algorithms for both line-of-sight (LOS) and non-line-of-sight (NLOS) conditions to solve the hyperbolic equations generated during fine-grained localization with TDOA. For analysis, [3] uses three anchor nodes arranged in a right-angled triangle with a slow-moving mobile node within the triangle formed by the anchor nodes. Since this setup is similar to that of GRADELOC and IGRADELOC, the results from [3] for LOS conditions are applied to define the approximate localization error expected during fine-grained localization. Therefore, for simulation purposes, the GetTDOALoc() function in our algorithm essentially returns the actual location with a certain error to account for localization inaccuracies.

In IGRADELOC, we introduce a parameter, fineCntLimit, which can be used to trigger an out-of-turn fine-grained localization if the computed centroid does not change after a specified number of centroid computation steps. The fineCntLimit is set based on the NTL's movement characteristics and the maximum expected duration for which the centroid may not change. If we consider Fig. 6, an NTL moving across CI,r1C_{I,r1} at a maximum speed SS will not change the centroid for a distance of 2(r1)2(r_1). Therefore, for a centroid computation interval of PP, 0<fineCntLimit≤|2(r1)PS|0 < \text{fineCntLimit} \leq \left| \frac{2(r_1)}{PS} \right| is used, provided 2(r1)PS≥1\frac{2(r_1)}{PS} \geq 1. To avoid out-of-turn localization, an excessively large value for fineCntLimit is chosen.

2. Self-localization with mobility module

We can accurately calculate displacement as described in [2] and [1]. However, the displacement cannot be used for localization unless the initial position error is eliminated. Therefore, for the results of GetACCELLoc() to be meaningful, it is necessary for an EFG-NTL to have both fineGrained and selfLocalize enabled, as shown in Table 1. In [1], the authors report on an experimental Pedestrian Navigation System, where they use accelerometer-based step and stride information, along with a gyroscope and magnetic compass combination for heading determination. We adopt a similar model, as shown in Fig. 7, where the EFG-NTL is assumed to be a pedestrian equipped with a module containing an accelerometer, gyroscope, and magnetic compass.

For the analysis, we assume that all three sensors are error-prone. The accelerometer reports the stride length as a percentage SASA of the actual length, and step detection is governed by a percentage DADA. In our deployment scenario, which follows a square grid, the NTL starts at the top-left corner and moves toward the bottom-right corner of the grid. It randomly selects a direction (either right or down) after every NN steps it takes in a particular direction. A heading error of θ∘\theta^\circ is introduced when the NTL moves right (or downwards) in the specified direction.

8. SIMULATION

A discrete-event simulation of theproposed algorithm is carried out with the parameters given in the following sub-sections. The behaviour of an NTLis analyzed by configuringit as a CG- NTL, FG-NTL and EFG-NTL by setting the parameters as per Tab. 1.

Table2: Mapping of Error Index to Range

ErrorIndex	e(AbsoluteErrorinm)
1	0≤e≤2
2	0≤e≤5
3	0≤e≤10
4	0≤e≤20
5	0≤e≤30
6	0≤e≤50
7	0≤e≤75

Table3:NTLType

Index	NTLType
1	CG-NTL
2	FG-NTL-Improved
3	FG-NTL
4	EFG-NTL-Accurate
5	EFG-NTL-Inaccurate

1. Topology, Beaconing and radio parameters

A set of25 nodes are arranged on afixed-gridina300mx300mfieldwith Lset to75mwhich makes our desirable node range ≥ 84m, a realistic assumption for commonly available nodes. Taking L= 75m and S = 1s, Eqn. 6 gives us 8.85 as the

value of P. A (close) value 10 is taken for P. Beacon interval p is 1 to achieve a granularity of 0.1. Threshold T is set to 0.9 (for both coarse-grained and fine grained). Each node has a transmission range of 84m. The Radio data- rate is 250 kbps with PSK as the modulation mechanism. Interference is used for collision detection at the receiver.

2. Parameter for fine-grained localization of (E)FG-NTL

AsoutlinedinSec.7.1Taylor-seriesmethodandFang'smethodunderLOSconditionsresultin errors in the rangeof(1m-5.5m)and(1m-7m)respectively.TheresultfromFang'smethodis used to estimate the error in fine-grained localization since it gives us a higher upper bound of the localization error. Essentially, the location (x,y) computed by GetTDOALoc() has an error givenby±(xerror,yerror)addedtotheactuallocation, whereboththeparametersareoutcomes oftwoindependentuniformpdfswith(qmin,qmax)as limits.Choosing±(1,5)asthevaluefor (qmin, qmax) gives us the minimum and maximum MAE of 1√2m(1.4m) and 5√2m(7m). Since S is 1m/s , P = 10 and r1 = L/2 = 37.5m, *fineCntLimit*is taken as 4 to stay within the bounds of the limits discussed in Sec. 7.1. This improved version of FG-NTL is henceforth referredtoasFG-NTL-Improved.ForanormalFG-NTL,*fineCntLimit*istypicallysetto100(a large value) to prevent an out-of-turn fine-grained localization.

3. A step, stride based NTL mobility model

Two sets of values are used for the mobility model. A set of values SA=95%,DA=99%,GA = 5°representsahighlyaccurateequipment where, SA=95%indicatesthatthereported stride length is 95% of the actual stride length, reported number of steps (DA) is 99% of the actual numberandaheadingerror(GA)of5°occursonthelinesoftheresultsshownin[2].TheEFG- NTL with these parameters is henceforth called EFG-NTL-Accurate. We also use set SA = 90%,DA = 90%, GA = 10° to observe the degradation in performance, with inaccurate hardwareandthecorrespondingEFG-NTLiscalledEFG-NTL-Inaccurate.Forallpurposes,the NTL takes one step per sec. Stride length SL (in m) of the step is determined by a uniformly distributed random variable in the range [0.7, 0.8].

9. RESULTS

1. Comparison of theoretical MAE and MAE obtained from simulation

The MAE for coarse-grained localization obtained from simulation as shown in Fig. 8isfound to agree with the theoretical error given by Eqn. 5 indicating that our analysis can be used for carrying out a pre-deployment network planning to determine the side length of each square grid-cell and the desirable radio range (which could be adjusted by possibly altering the transmission power level of the sensor node) to achieve the desired precision of coarse-grained localization.

2. Performance comparison of NTLs

Fig. 9 uses the error index from Table 2 to display the error distribution for CG-NTL, FG-NTL, FG-NTL-Improved, EFG-NTL-Accurate, and EFG-NTL-Inaccurate. It is observed that EFG-NTL-Accurate performs the best, with all errors within 10m (Error Index = 3), while CG-NTL shows the poorest performance, with less than 2% of errors within 10m. EFG-NTL-Inaccurate has 89% of errors within 10m. A significant improvement in performance is seen with FG-NTL-Improved, where 59% of errors are within 10m, compared to 47% for FG-NTL. The mean absolute error (MAE) and root mean squared error (RMSE) for all NTLs are presented in Fig. 10. The NTLType interpretation is provided in Table 3. FG-NTL-Improved has lower MAE and RMSE values than FG-NTL, with about 8% additional communication overhead.

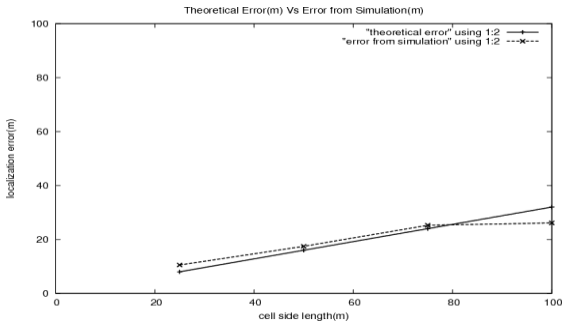

Figure8: A comparison of theoretical values for coarse-grained localization error and the corresponding values obtained from simulation

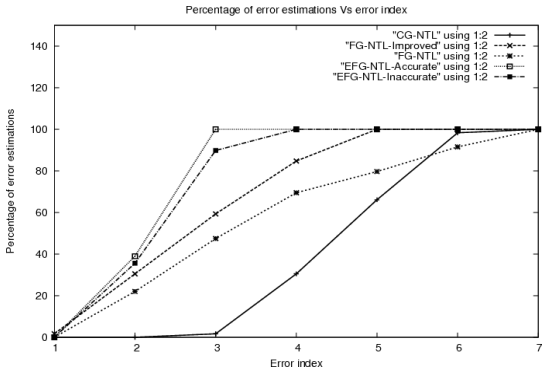

Figure9: Distribution of localization errors for various NTLs

10. ENERGY CONSIDERATIONS

With IGRADELOC, a part from graded expenditure of energy through design modularity, fine- grained localization initiation by notification of at least three REFN1s with a single broadcast from an NTL, and introduction of the *fine Cnt Limit* parameter for fine-tuning (localization) precision and cost(ofcommunication)helpsinfurtherregulatingth eenergyconsumption.EachNTLspendsenergyaccor dingtoitslevelofsophistication.CG-NTLsarejustpassivereceivers. FG-NTL spends some additional energy for notifying REFN1s for a fine-grained localization, and EFG-NTLs spend some energy (in addition to the amount spent by FG-NTL) on their mobility module.

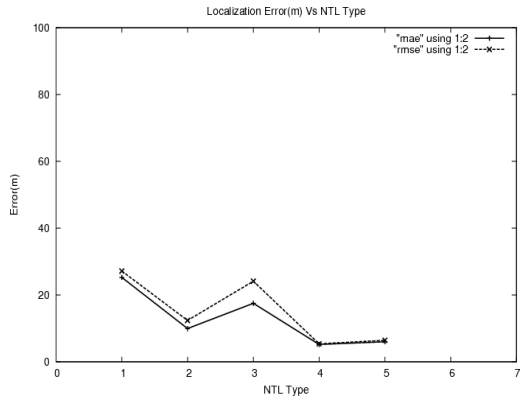

Figure10: MAE, RMSE of localization errors for various NTLs

11. CONCLUSION

In IGRADELOC, the focus has been on enhancing the performance of FG-NTLs and EFG-NTLs within a deployment architecture, highlighting their necessity. The characteristics of the topology, including grid-cell dimensions and the transmission range of REFN0 and NTL, have been analyzed to choose the optimal configuration for achieving the desired performance. Additionally, the architecture now includes routing capabilities through the grid nodes.

REFERENCES

[1] J. W. Kim, H. J. Jang, D. Hwang, and C. Park, A step, stride and heading determination for the pedestrian navigation system, Journal of Global Positioning Systems 3 (2004), no. 1-2, 273–279.

[2] L. Klingbeil and T. Wark, A wireless sensor network for real-time indoor localization and motion monitoring, Proc. of 7th Intl Conf. on Inf. Proc. in Sensor Networks, 2008, pp. 39–50.

[3] D. Ping, Yongjun, X., and L. Xiaowei, A robust location algorithm with biased extended kalman filteringoftdoa dataforwirelesssensor networks,Proc. ofIntlConf. onWirelessComm.,Networking& Mobile Computing (WCNM'05) (Wuhan, China), vol. 2, 2005, pp. 883–886.

[4] S. Sarangi and S. Kar, A novel algorithm for graded precision localization in wireless sensor networks, Proc. of 1st Intl. Conf. on Networks and Comm. (NETCOM'09) (Chennai, India), pp. 18–22, 2009.

[5] Sarangi, S., & Kar, S. (2010). Performance Analysis of an Improved Graded Precision Localization Algorithm for Wireless Sensor Networks. *International Journal of Computer Networks & Communications (IJCNC)*, 2(4), 133–145. doi: 10.5121/ijcnc.2010.2413.

[6] Gokhale, P., & Patil, R. (2017). A review of localization algorithms for wireless sensor networks. *International Journal of Computer Applications*, 170(6), 1–6. doi: 10.5120/ijca2017912421.

[7] Zhang, Z., & Xu, C. (2019). Survey on localization algorithms in wireless sensor networks: From theory to practice. *Sensors*, 19(20), 4447. doi: 10.3390/s19204447.

[8] Liu, X., & Shen, Y. (2020). An improved localization algorithm for wireless sensor networks based on hybrid positioning. *Wireless Personal Communications*, 114(1), 449–465. doi: 10.1007/s11277-020-07435-4.

[9] Pompili, D., & Xie, L. (2012). A survey on localization algorithms for wireless sensor networks. *IEEE Access*, 1, 1337–1348. doi: 10.1109/ACCESS.2013.2261982.

[10] Arshad, Z., & Khalil, A. (2018). Localization in wireless sensor networks: A comprehensive review. *International Journal of Distributed Sensor Networks*, 14(5), 1–13. doi: 10.1177/1550147718774875.

[11] Shen, Z., & Zhang, X. (2015). A novel hybrid localization algorithm for wireless sensor networks. *International Journal of Communication Systems*, 28(9), 1740–1754. doi: 10.1002/dac.2909.